https://doi.org/10.5194/egusphere-2023-2564
Preprint. Discussion started: 16 November 2023
© Author(s) 2023. CC BY 4.0 License.

Chaetoceros resting spores record low diatom-bound nitrogen isotope values: Evidence from laboratory culture and marine sediment

Isabel A. Dove[1], Ian W. Bishop[1], Xavier Crosta[2], Natascha Riedinger[3], R. Patrick Kelly[1], Rebecca S. Robinson[1]

[1]Graduate School of Oceanography, University of Rhode Island, Narragansett, RI, USA
[2]UMR-CNRS 5805 EPOC, University of Bordeaux, Pessac, France
[3]Boone Pickens School of Geology, Oklahoma State University, Stillwater, OK, USA

Correspondence to: Isabel A. Dove (isabel_dove@uri.edu)

Abstract. The nitrogen isotopic composition of diatom frustule-bound organic matter ($\delta^{15}N_{DB}$) is often used to study changes in high latitude biological pump efficiency across glacial-interglacial cycles, but the proxy may be biased by species-specific effects. The genus *Chaetoceros* is of particular interest because of its abundance throughout ocean basins, its shifting biogeography during glacial periods, and many species' ability to form heavily silicified resting spores. Here we investigate how *Chaetoceros* resting spores (CRS) record surface nitrate conditions in their nitrogen isotopic composition using both laboratory culture experiments and assemblage-specific sedimentary $\delta^{15}N_{DB}$ measurements. We find that CRS record $\delta^{15}N_{DB}$ values 7.0 ± 2.6‰ lower than vegetative *Chaetoceros* in culture and 5.6 ± 1.9‰ lower than non-CRS diatoms in sediment. Low values are attributed to assimilation of isotopically light ammonium, heavy silicification, and internal fractionation during sporulation. Despite the large $\delta^{15}N_{DB}$ difference observed in CRS versus non-CRS diatoms, increased CRS relative abundance in open ocean glacial sediments does not significantly bias $\delta^{15}N_{DB}$ records due to the spores' small size.

1 Introduction

Modulations in high-latitude biological pump efficiency have long been recognized as a potential driver of glacial-interglacial cycles (Knox & McElroy, 1984; Sarmiento & Toggweiler, 1984), with fossil-bound nitrogen (N) isotope records suggesting that a more efficient biological pump played a role in lowering glacial atmospheric CO_2 (Ai et al., 2020; Martínez-García et al., 2014; Robinson et al., 2005; Robinson & Sigman, 2008; Sigman et al., 1999; Studer et al., 2015). However, these records are limited by uncertainties around species-related influences (e.g., Horn et al., 2011b) and geographic coverage, as there are no published records from highly productive regions proximal to the Antarctic coast. Characterizing species- or genus-specific biases in fossil-based proxy records is critical to ensuring sound comparisons between oceanic regions with differing community assemblages.

https://doi.org/10.5194/egusphere-2023-2564
Preprint. Discussion started: 16 November 2023
© Author(s) 2023. CC BY 4.0 License.

Within the Antarctic Zone (AZ) of the Southern Ocean (Fig. 1), wind-driven upwelling brings nutrient- and CO_2-rich waters to the surface, where nutrients are incompletely utilized by phytoplankton due to iron and light limitation (Martin, 1990; Mitchell et al., 1991). This incomplete nutrient utilization results in inefficient export and sequestered CO_2 leaking back into the atmosphere (Sigman et al., 2010). Changes in relative nutrient utilization in the nitrate-replete AZ, and therefore changes in biological pump efficiency, can be investigated via sedimentary N isotope records. The isotopic composition of N ($\delta^{15}N$) in sediments reflects the preferential uptake of nitrate containing ^{14}N by phytoplankton, leaving behind a nutrient pool enriched in ^{15}N-containing nitrate (Wada and Hattori, 1978). As nitrate consumption progresses, the nitrogen isotopic composition of both the nitrate pool and the resulting organic matter becomes progressively enriched in ^{15}N, with the higher $\delta^{15}N$ value of sinking organic matter reflecting enhanced nitrate utilization (Altabet and Francois, 1994). Because the $\delta^{15}N$ of bulk organic particles may be altered during sinking and after sedimentation, fossil-bound N isotope records, which represent organic N bound with biominerals and purportedly protected from alteration, are preferred for paleoceanographic analyses (Robinson et al., 2004, 2020; Sigman et al., 1999).

Diatoms, which are single-celled algae characterized by their opaline frustules, are the ideal microfossil group with which to generate fossil-bound $\delta^{15}N$ records in the Southern Ocean due to their abundance in surface water and in sediments. Diatoms are the dominant type of phytoplankton in the AZ and are primary contributors to the Southern Ocean biological pump (Smetacek et al., 2012; Rigual-Hernández et al., 2015). The efficiency with which diatoms export carbon depends on many factors including size and morphology (Tréguer et al., 2018), along with the aforementioned effect of nutrient supply. While diatom frustules are primarily composed of biogenic silica, they contain structural proteins and polyamines that comprise the N pool from which diatom-bound N isotopes ($\delta^{15}N_{DB}$) are measured (Sumper and Kröger, 2004; Kröger et al., 1999, 2000; Hildebrand et al., 2018).

Despite its proven utility, the $\delta^{15}N_{DB}$ proxy may suffer from species-specific biases. Sedimentary $\delta^{15}N_{DB}$ records integrate N fractionation signals from all diatom species present in a given sample and therefore may be affected by community composition (Jacot Des Combes et al., 2008; Horn et al., 2011b; Studer et al., 2013, 2015). Different diatom species contain varying proportions of N-bearing organic compounds with distinct fractionations and thus isotopic compositions within their frustules, resulting in a possible species-specific relationship between $\delta^{15}N_{biomass}$ and $\delta^{15}N_{DB}$ (Horn et al., 2011a; Jones et al., 2022). The offset between $\delta^{15}N_{biomass}$ and $\delta^{15}N_{DB}$ of a given species is represented by ε_{DB}, signifying differences in how diatoms fractionate N into their frustules' organic matrices. Recent field and culture work suggest negative values of ε_{DB} ($\delta^{15}N_{biomass} < \delta^{15}N_{DB}$), with species-specific offsets related to cellular Si:N allocation (Jones, 2020; Robinson et al., 2020). Therefore, it is critical to further examine how the $\delta^{15}N_{DB}$ of certain diatom species relates to the surface nutrient conditions of the ocean in which they grew.

https://doi.org/10.5194/egusphere-2023-2564
Preprint. Discussion started: 16 November 2023
© Author(s) 2023. CC BY 4.0 License.

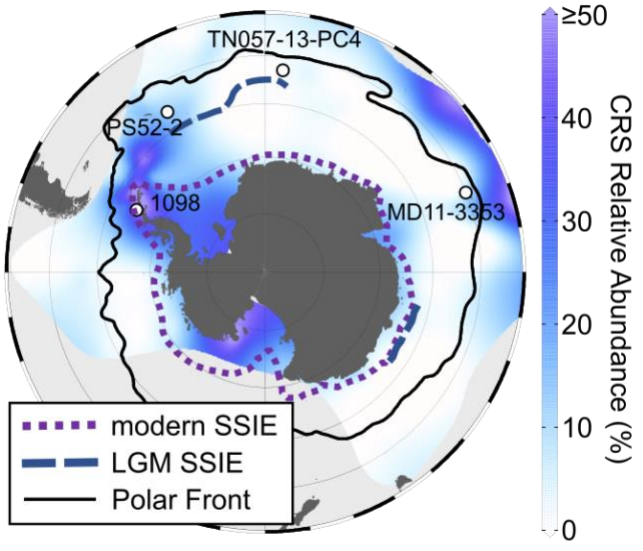

Figure 1: Relative abundance (%) of CRS in modern Southern Ocean sediments (Esper et al., 2010; Armand et al., 2005; Crosta et al., 1997) and location of sediment cores PS119 Site 52-2, ODP Site 1098, TN057-13-PC4, and MD11-3353. Grey shading indicates regions with no CRS data. Dashed blue lines indicate the summer sea ice edge (SSIE) during the last glacial maximum (Gersonde et al., 2005), dotted purple line indicates the modern summer sea ice edge (Schweitzer, 1995), and solid black line represents the northern boundary of the modern Antarctic Zone (Orsi et al., 1995).

The diatom genus *Chaetoceros* is particularly relevant because it is a prominent component of Southern Ocean diatom assemblages, particularly in coastal areas, and plays an important role in exporting carbon to the deep ocean (Rembauville et al., 2016). Many species of the *Chaetoceros* subgenus *Hyalochaete* form robust resting spores (herein CRS) as a survival strategy in response to adverse conditions such as nutrient or light limitation (French and Hargraves, 1985; Oku and Kamatani, 1997; Pelusi et al., 2020). In contrast to weakly silicified vegetative valves of *Chaetoceros* subg. *Hyalochaete*, CRS are heavily silicified. Laboratory-based experiments show that frustule dissolution may bias Southern Ocean sedimentary diatom assemblages, with vegetative *Chaetoceros* frustules being more readily dissolved than resting spores (Crosta et al., 1997; Pichon et al., 1992). Additionally, sediment trap records from both the North Atlantic and the Southern Ocean show that the relative proportion of resting spores within sinking diatom assemblages increases with depth due to enhanced preservation of robust frustules (Rynearson et al., 2013; Rembauville et al., 2016). Because CRS likely form under nutrient-depleted conditions (in which nitrate is enriched in ^{15}N) and because they are preferentially preserved in marine sediments, we hypothesize that they bias records towards higher $\delta^{15}N_{DB}$ values, which signal a greater degree of nutrient utilization.

https://doi.org/10.5194/egusphere-2023-2564
Preprint. Discussion started: 16 November 2023
© Author(s) 2023. CC BY 4.0 License.

CRS microfossils are common in Southern Ocean marine sediments and are associated with coastal settings both around Antarctica and subantarctic islands, but their relative abundance varies across time and space (Armand et al., 2005; Crosta et al., 1997; Esper et al., 2010; Zielinski & Gersonde, 1997; Fig. 1). Around Antarctica, they are associated with sea ice, as modern sediment trap data show blooms co-occurring with melting sea ice in the austral spring (Leventer, 1991). Furthermore, laminated coastal sediments suggest CRS following sea ice retreat (Denis et al., 2006; Maddison et al., 2005). Importantly, the relative abundance of CRS increases in pelagic sediments and offshore of subantarctic islands during glacial intervals due to the northward extent of the sea ice edge (Abelmann et al., 2006). Therefore, increased CRS relative abundance in glacial sediments could bias Antarctic Zone $\delta^{15}N_{DB}$ records spanning glacial-interglacial cycles.

Here we present the results of laboratory culture experiments in which wild type *C. socialis* were resurrected from resting spores in Southern Ocean surface sediment and induced back into resting spores by nitrate limitation to characterize how CRS record surface nutrient conditions in their N isotopic composition. We supplement our culture work with analysis of $\delta^{15}N_{DB}$ measured from isolated sedimentary CRS and apply our findings to reevaluate relevant published $\delta^{15}N_{DB}$ records, with accompanying diatom assemblage data, spanning glacial-interglacial cycles. Contrary to expectations, we find that CRS record low $\delta^{15}N_{DB}$ values relative to biomass and vegetative cells, potentially skewing $\delta^{15}N_{DB}$ measurements towards lower values and therefore leading to underestimates of the role of the biological pump in lowering glacial atmospheric CO_2. Mass balance calculations using published diatom community assemblages over glacial-interglacial cycles and biometric data suggest that only large changes in CRS relative surface area contribution significantly bias $\delta^{15}N_{DB}$ records.

2 Materials and Methods

2.1 Laboratory cultures

2.1.1 Culture material

Spore-forming *Chaetoceros* diatoms were grown in culture and induced into resting spores to characterize how CRS record nutrient utilization in their nitrogen isotopic composition. Strains of spore forming *Chaetoceros* were obtained by isolating vegetative cells that germinated from sedimentary resting spores. Resting spore-rich surface sediments were retrieved by a multicore at site 52-2 of the RV *Polarstern* expedition PS119 (Bohrmann, 2019) in the Scotia Sea (56.14 °S, 31.48 °W, 3,359 m water depth; Fig. 1) and were stored in 50 mL centrifuge tubes in a dark refrigerator.

To induce germination, 1 mL of resting spore-rich sediment slurry was pipetted into 5 mL of sterile filtered f/2 medium (Guillard, 1975). This inoculant was diluted by pipetting 500 µL into another well with 5 mL of f/2. The resting spores were kept in a 4 °C incubator at 24-hour continuous light (50-70 µmol photons m^{-2} s^{-1}) and were periodically stirred gently and monitored for germination by light microscopy. Germination typically occurred within 4-8 weeks. Cells were then isolated in

https://doi.org/10.5194/egusphere-2023-2564
Preprint. Discussion started: 16 November 2023
© Author(s) 2023. CC BY 4.0 License.

well plates and transferred to progressively larger volumes while in exponential growth phase. All experiments were conducted with strains of *C. socialis*, which were visually identified to the species level (Hasle and Syvertsen, 1997). Identification was confirmed by 18S rDNA sequence following the method of Bishop et al. (2022), the only difference being that rDNA was extracted using the Zymo Quick-DNA/RNA Miniprep Plus Kit, following the manufacturer's protocol. *Chaetoceros socialis* is an ideal species with which to investigate the genus *Chaetoceros* because, within the genus, *C. socialis* is both the most abundant species and contributes the largest percentage to global diatom biomass (Leblanc et al., 2012).

2.1.2 Culture experiments

Three experiments, each in triplicate, were conducted to characterize the nitrogen isotopic composition of vegetative *Chaetoceros* and CRS. Culture experiments were conducted in 20 L carboys to ensure sufficient material for $\delta^{15}N_{DB}$ measurements. Carboys were filled with about 20 L of sterile filtered (0.2 μm) seawater from Narragansett Bay. Phosphate, silicic acid, trace metals, and vitamins were added at f/2 concentrations, while nitrate was restricted to 45 μM concentrations to induce resting spore formation. Previous studies have induced CRS formation with nitrate concentrations between 10 and 23 μM, but we increased the concentration to obtain more material for $\delta^{15}N_{DB}$ measurements (Kuwata et al., 1993; Oku & Kamatani, 1997; Pelusi et al., 2020). Each carboy was inoculated with 200 mL of culture in exponential growth phase. Since the inoculant was grown in f/2 medium, initial nutrient concentrations in the three carboys varied slightly and nitrate concentrations exceeded 45 μM. Cultures were kept at 4 °C with 24-hour continuous light to simulate summertime Southern Ocean conditions and were continuously stirred and bubbled with filtered air. Cell growth was tracked via fluorescence and water samples were collected periodically throughout the experiment to track nutrient (silicic acid, ammonium, nitrate) utilization (Fig. 2). Water samples were filtered and stored frozen until analysis, with subsamples acidified to pH 2 for ammonium concentration measurements. Approximately 5 mL of unfiltered water samples were also collected and preserved in a 2% acid Lugol's solution to monitor resting spore abundance. Cell counts were performed using a Sedgewick Rafter and a Nikon Eclipse E800 compound microscope under 200x magnification, with a minimum of 500 cells counted per sample.

We investigated the nitrogen isotopic composition of both vegetative *Chaetoceros* and CRS by harvesting cultures at two timepoints: before and after resting spore formation. Vegetative samples were collected by filtering biomass from approximately 10 L of each carboy prior to resting spore formation, 6-7 days after inoculation. Subsamples of 50 mL were filtered onto a precombusted GF/F filter for $\delta^{15}N_{biomass}$ measurements. The remaining volume was filtered with 5 μm polycarbonate filters for $\delta^{15}N_{DB}$ measurements. All filters were kept frozen until analysis. Once a significant proportion of cells had sporulated, approximately 30 days later, CRS were harvested following the same procedure. The timing of sampling for each experiment is described in the Supplement.

https://doi.org/10.5194/egusphere-2023-2564
Preprint. Discussion started: 16 November 2023
© Author(s) 2023. CC BY 4.0 License.

2.1.3 Dissolved silica measurements

Frozen water samples were gently thawed over a 24-hour period to avoid Si precipitation prior to dissolved silica (dSi) analysis. The dSi concentration was measured with a UV/Vis spectrophotometer following the colorimetric method of Strickland & Parsons (1972). Given high dSi concentrations in f/2 medium, water samples collected early in the experiment were diluted to lower concentrations. Concentrations were calibrated with a sodium silicate dilution series ranging from 1.25-50 µM and accuracy verified with the KANSO lot CH certified reference material. Analytical precision, as determined by the pooled standard deviation of multiple measurements of replicate samples, is 0.9 µM.

2.1.4 Ammonium concentration measurements

Acidified water samples were analyzed for ammonium concentration following the fluorometric method of Holmes et al. (1999). 2 mL of each water sample was added to 8 mL of working reagent and incubated in the dark for 4 hours. Fluorescence was measured with the CDOM/NH_4 optical package on a Turner Designs Trilogy Laboratory Fluorometer. Concentrations were calibrated with an ammonium chloride dilution series ranging from 0.25-5.0 µM. Analytical precision is 0.4 µM.

2.1.5 Nitrate concentration and isotope analysis

Nitrate concentration in water samples was measured by chemiluminescent NO detection after conversion with a heated vanadium reagent using a Teledyne Instruments Model 200E chemiluminescence NO/NO_x analyzer (Braman and Hendrix, 1989). The nitrogen isotopic composition of nitrate ($\delta^{15}N_{NO3}$) was measured via the denitrifier method, in which nitrate is converted to nitrous oxide by denitrifying bacteria (Sigman et al., 2001). The $\delta^{15}N_{NO3}$ isotope ratio was measured by gas chromatography-isotope ratio mass spectrometry on a Thermo Delta V IRMS and measurements were standardized with potassium nitrate reference materials IAEA-N3 and USGS34. Analytical precision is 0.2‰.

2.1.6 Total reduced nitrogen concentration and isotope analysis

Reduced nitrogen (ammonium and dissolved organic nitrogen) in water samples was oxidized to nitrate following a modified persulfate oxidation method (Knapp et al., 2005). A volume of 250 µL of a 0.22 M potassium persulfate and 1.5 M sodium hydroxide solution was added to 1.5 mL of water sample and reacted in a pressure cooker (118°C) for one hour. Known amounts of the amino acid, glycine, were processed identically to ensure complete oxidation of reduced nitrogen. Following persulfate oxidation, nitrate concentration was measured by chemiluminescent NO detection. Total reduced nitrogen concentration was calculated by subtracting previously measured nitrate concentrations.

https://doi.org/10.5194/egusphere-2023-2564
Preprint. Discussion started: 16 November 2023
© Author(s) 2023. CC BY 4.0 License.

The nitrogen isotopic composition of oxidized samples was measured via the denitrifier method. A mass balance calculation using nitrate concentrations and $\delta^{15}N_{NO3}$ values from un-oxidized samples yielded the nitrogen isotopic composition of reduced nitrogen. Analytical precision is 0.3‰.

2.1.7 Biomass N isotope analysis

Dried GF/F filters were wrapped in tin capsules for $\delta^{15}N_{biomass}$ analysis with a Costech 4010 elemental analyzer coupled to a Thermo Delta V IRMS. Measurements were calibrated using reference materials IAEA N1 and N2 as well as an in-house aminocaproic acid standard. Analytical precision is 0.3‰.

2.1.8 Culture diatom-bound N isotope analysis

Vegetative and CRS samples were chemically cleaned for $\delta^{15}N_{DB}$ analysis following the method of Morales et al. (2013). First, samples were repeatedly rinsed with a 2% sodium dodecyl sulfate (SDS) solution to remove weakly bound organic matter. Next, external organic matter was removed by permanganate oxidation, using sulfuric acid, saturated potassium permanganate, and saturated oxalic acid solutions. Finally, samples were treated with weak and strong perchloric acid solutions in a 100 °C water bath to remove any remaining external organic matter.

Since frustules from dead vegetative cells remain in the carboys when the CRS sample is collected (Fig. 2), additional treatment was required to isolate CRS. During the first two of the three culture experiments, we were unable to isolate CRS, instead collecting mixed vegetative and CRS samples. CRS were successfully isolated for $\delta^{15}N_{DB}$ analysis during the third experiment. Following the SDS rinse, CRS samples were sonicated at 80 kHz to break the more fragile vegetative frustules. The sonicated samples were then filtered through a 5 µm Nitex mesh. The >5 µm fraction was left to settle in a 250 mL beaker filled with water for two hours. The samples were siphoned to ~40 mL, where only CRS remained (Fig. S1).
Following chemical cleaning, dry samples were dissolved in a 0.22 M potassium persulfate and 1.5 M sodium hydroxide solution and organic frustule-bound N was oxidized to nitrate (Robinson et al., 2004). Nitrate concentrations were measured by chemiluminescent NO detection and $\delta^{15}N_{DB}$ values were measured by the denitrifier method, as described above. Small sample sizes preclude duplicate CRS samples, but duplicate measurements of vegetative samples yield 0.4‰ analytical precision.

2.2 Sedimentary CRS analysis

Sedimentary CRS were analyzed to supplement laboratory results with a field-based view of how CRS record surface ocean nutrient conditions in their nitrogen isotopic composition. Laminated deglacial sediments at ODP Site 1098 (64°51’ S, 64°12’ W, 1012 m depth; Fig. 1) contain nearly monogeneric layers of CRS deposited during the austral spring (Maddison et al., 2005). We measured $\delta^{15}N_{DB}$ from both the bulk diatom assemblage and isolated CRS within six CRS-rich spring laminae to ensure that differences in $\delta^{15}N_{DB}$ are due to diatom assemblage rather than seasonal changes in surface ocean nutrients.

https://doi.org/10.5194/egusphere-2023-2564
Preprint. Discussion started: 16 November 2023
© Author(s) 2023. CC BY 4.0 License.

2.2.1 Sedimentary diatom-bound N isotope analysis

All sedimentary $\delta^{15}N_{DB}$ samples were sieved at 63 μm, using the <63 μm fraction for the bulk diatom assemblage $\delta^{15}N_{DB}$ measurements. Samples for CRS-specific $\delta^{15}N_{DB}$ measurements were further processed following the methods of Egan et al. (2012) and Swann et al. (2013). Subsamples of the <63 μm fraction were filtered through a 10 μm Nitex mesh in a gentle ultrasonic bath. The resulting <10 μm fraction was dominated by CRS, but vegetative *Chaetoceros* were also present in similar proportions as in unseparated samples (Fig. S2).

Both the bulk diatom assemblage and isolated CRS samples were prepared for $\delta^{15}N_{DB}$ analysis following the method described in Horn et al. (2011b). The method is almost identical to that previously described for culture $\delta^{15}N_{DB}$, with the exception of omitting the SDS rinse and adding a reductive cleaning step to remove adsorbed metals with a sodium dithionite solution. Similar to the culture samples, cleaned sedimentary samples were dissolved and $\delta^{15}N_{DB}$ values were measured by the denitrifier method. Analytical precision is 0.4‰.

2.2.2 Diatom community composition and surface area analysis

To assess how CRS bias sedimentary $\delta^{15}N_{DB}$ records, it is essential to consider the relative amount of organic nitrogen that CRS contribute to the bulk diatom assemblage N pool. While CRS dominate the diatom assemblage in terms of relative numerical abundance, they are much smaller than other diatoms within the deglacial sediments from Site 1098, such as *Corethron* spp., *Coscinodiscus* spp., and *Thalassiosira antarctica* (Maddison et al., 2005; Taylor and Sjunneskog, 2002). Therefore, relative surface area is a more accurate measure of CRS contribution to the $\delta^{15}N_{DB}$ signal than relative abundance. CRS contribution was quantified in terms of both relative surface area and relative abundance. Quantitative microscope slides of the <63 μm fraction were made following the method of Scherer (1994). The two-dimensional surface area of all diatoms and of only CRS was measured following the method of Studer et al. (2013), in which 20 photomicrographs were taken at random for each sample at 400x magnification. Total diatom surface area and CRS-specific surface area was determined by manually selecting CRS and all other diatoms using ImageJ software. Diatom community composition was determined by identifying and counting at least 400 diatom valves at 1000x magnification, following the technique of Crosta & Koç (2007). The CRS relative contribution for each sample was calculated by dividing CRS surface area or abundance by total diatom surface area or abundance.

https://doi.org/10.5194/egusphere-2023-2564
Preprint. Discussion started: 16 November 2023
© Author(s) 2023. CC BY 4.0 License.

3 Results

3.1 Culture growth, spore formation, and nutrient utilization

Due to insufficient separation of CRS from vegetative frustules following the first two experiments, the data presented below result from the third experiment, unless otherwise noted. Data from the first two experiments can be found in the Supplement.

Experiment 3 cultures grew exponentially until day 6, when vegetative cells were harvested (Fig. 2). Fluorescence decreased following nitrate depletion and the onset of resting spore formation. Resting spores first appeared on day 7 in carboys 1 and 3 and on day 6 in carboy 2. Spore formation continued until harvesting on day 36, with approximately 17% of cells sporulating (Table 1).

Table 1: Cell counts from experiment 3.

	Cells/L	CRS/L	%CRS
C1 veg. harvest	7.4×10^7	0	0
C2 veg. harvest	7.3×10^7	2.9×10^6	3.9
C3 veg. harvest	1.1×10^8	0	0
C1 CRS harvest	4.2×10^7	7.4×10^6	17.4
C2 CRS harvest	4.8×10^7	8.5×10^6	17.9
C3 CRS harvest	3.7×10^7	6.1×10^6	16.8

The dSi concentrations initially averaged 40.7 ± 1.4 µM and decreased to full depletion by day 11 (Fig. 2). When vegetative cells were harvested on day 6, just prior to sporulation, dSi concentrations averaged 30.6 ± 1.1 µM.

Average initial nitrate concentrations were 44.7 ± 3.4 µM with an average $\delta^{15}N_{NO3}$ value of 9.6 ± 0.4‰. Nitrate was fully depleted by day 5 and $\delta^{15}N_{NO3}$ values increased with progressive consumption (Fig. 2). Ammonium concentration was initially 2.3 ± 0.7 µM and fully depleted by day 4. Concentrations then increased and oscillated between ~1-3 µM throughout the remainder of the experiment (Fig. 2). Total reduced N concentrations oscillate between ~30-50 µM (Fig. S3), with $\delta^{15}N$ values ranging between -2‰ and 3‰ (Fig. 2).

https://doi.org/10.5194/egusphere-2023-2564
Preprint. Discussion started: 16 November 2023
© Author(s) 2023. CC BY 4.0 License.

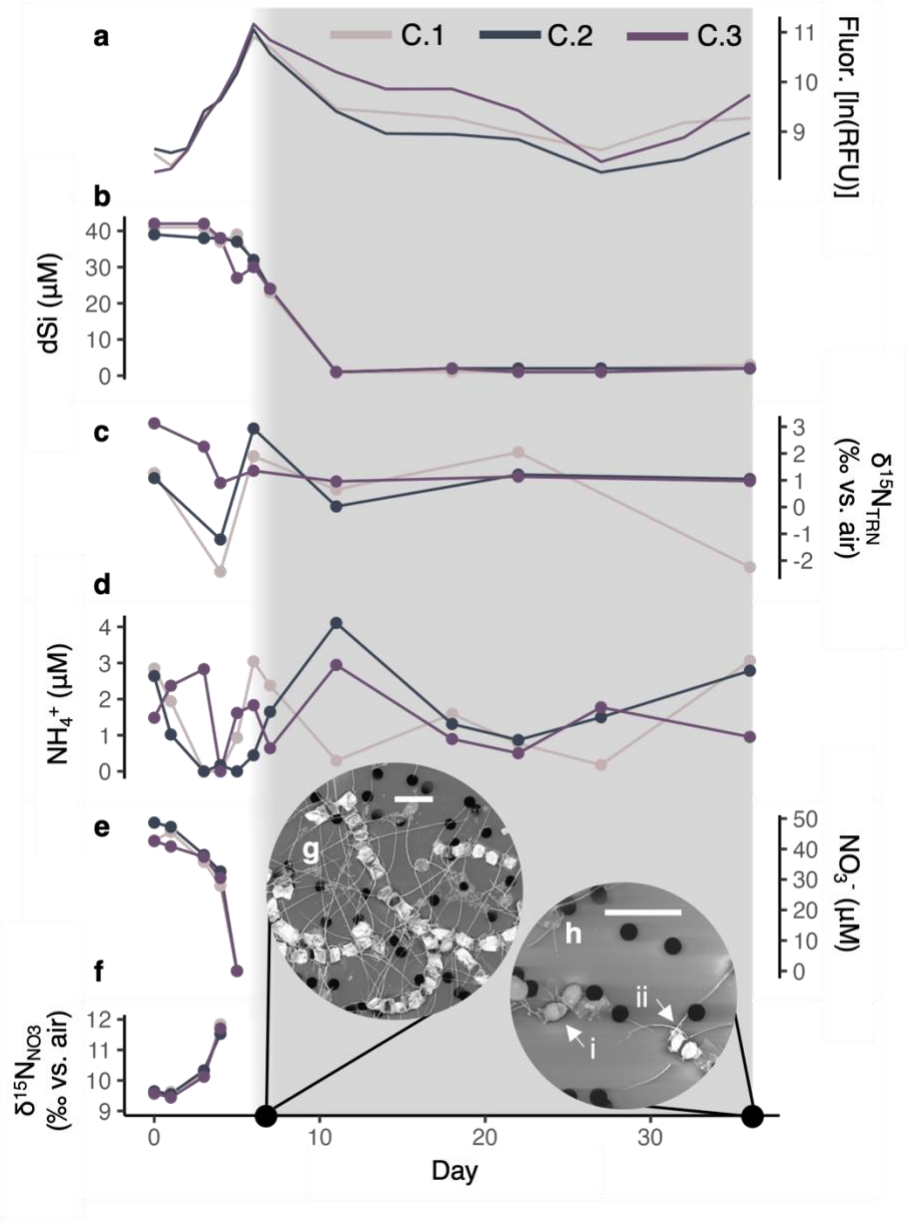

Figure 2: Culture growth and nutrient data tracked throughout experiment 3, color-coded by carboy (C.1-C.3). Growth is tracked via fluorescence and peaks when vegetative cells are harvested for isotopic analysis (a). Nutrients include dissolved Si (b), ammonium (d), and nitrate (e). The nitrogen isotopic composition of total reduced N (c) remains relatively constant while nitrate becomes progressively enriched in ^{15}N (f). Grey shading indicates presence of CRS and the black circles denote the days when vegetative cells and resting spores are harvested. Insets are SEM images of culture subsamples collected on the days in which vegetative cells (g) and CRS (h) were harvested. Both CRS (h.i) and frustules from dead vegetative cells (h.ii) are present when CRS cultures are harvested. Scale bars are 20 µm.

https://doi.org/10.5194/egusphere-2023-2564
Preprint. Discussion started: 16 November 2023
© Author(s) 2023. CC BY 4.0 License.

3.2 Biomass and diatom-bound $\delta^{15}N$

Average $\delta^{15}N_{biomass}$ is 8.1 ± 0.8‰ for harvested vegetative cells and 6.8 ± 0.9‰ for mixed vegetative cells and CRS (Fig 3). Since the carboys contained dead vegetative cells in addition to CRS, it is impossible to measure the $\delta^{15}N$ of biomass exclusively from CRS. The average $\delta^{15}N_{biomass}$ value of 8.1 ± 0.8‰ for harvested vegetative cells meets expectations given that all nitrate with an initial $\delta^{15}N_{NO3}$ value of 9.6 ± 0.4‰, plus some amount of reduced nitrogen with a low $\delta^{15}N$ value, is consumed.

Average $\delta^{15}N_{DB}$ for vegetative *Chaetoceros* is 6.5 ± 1.7‰. The $\delta^{15}N_{DB}$ value from carboy 2, in which CRS formation had already begun at the time of harvesting, is approximately 3‰ lower than the values from carboys 1 and 3, which together average 7.5 ± 0.3‰. The $\delta^{15}N_{DB}$ values for CRS in carboys 2 and 3 are -2.8 ± 0.4‰ and -0.5 ± 0.4‰, respectively (Fig 3). No $\delta^{15}N_{DB}$ value was measured from carboy 1 due to insufficient sample size following CRS isolation.

Across all experiments and adjusted to a single initial $\delta^{15}N_{NO3}$ value, average $\delta^{15}N_{DB}$ values for vegetative *Chaetoceros* is 10.0 ± 2.2‰. Mixed vegetative and CRS samples from the first two experiments and from carboy 2 of experiment 3 have an average $\delta^{15}N_{DB}$ value of 8.9 ± 2.9‰.

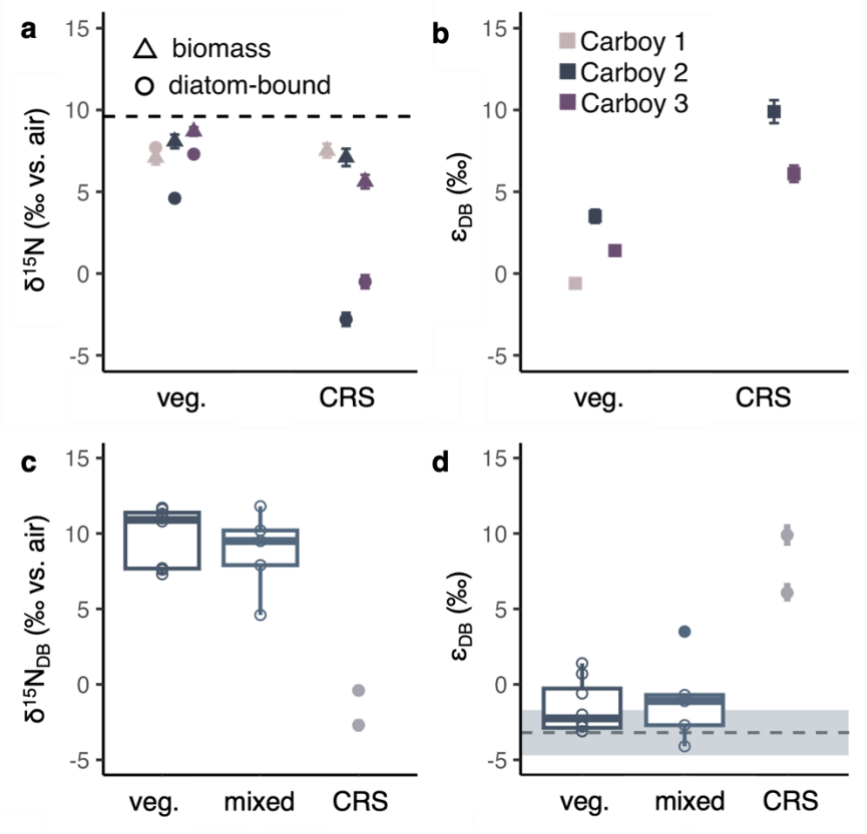

https://doi.org/10.5194/egusphere-2023-2564
Preprint. Discussion started: 16 November 2023
© Author(s) 2023. CC BY 4.0 License.

Figure 3: Isotope measurements and ε_{DB} calculations from culture experiments. Panels (a) and (b) show data from experiment 3, color-coded by carboy, while panels (c) and (d) show data from all experiments. The nitrogen isotopic composition of vegetative *Chaetoceros* frustules is enriched in ^{15}N relative to CRS (a). The dotted black line denotes the average initial $\delta^{15}N_{NO3}$ value of 9.6‰. Circles represent $\delta^{15}N_{DB}$ measurements and triangles represent $\delta^{15}N_{biomass}$ measurements. These measurements are used to calculate the ε_{DB} values ($\delta^{15}N_{biomass} - \delta^{15}N_{DB}$) shown in panel (b). $\delta^{15}N_{DB}$ measurements (c) and ε_{DB} calculations (d) for vegetative cells from all experiments (n=8) and mixed samples from the first two experiments plus carboy 2 of experiment 3 (n=5) are presented as boxplots. $\delta^{15}N_{DB}$ values from all experiments are adjusted to a single initial $\delta^{15}N_{NO3}$ value. CRS $\delta^{15}N_{DB}$ and ε_{DB} values are plotted as points because CRS are successfully isolated from two carboys during experiment 3. The dotted grey line and grey shading indicate average ε_{DB} (-3.2 ± 1.5‰) in the Antarctic Zone of the Southern Ocean (Robinson et al., 2020). CRS ε_{DB} is higher than that of vegetative *Chaetoceros* and ε_{DB} measured in the field (d).

3.3 Sedimentary $\delta^{15}N_{DB}$ and diatom community assemblage

The average $\delta^{15}N_{DB}$ value for the entire <63 μm diatom community ($\delta^{15}N_{DB\text{-}bulk}$) is 9.3 ± 0.6‰, while the average $\delta^{15}N_{DB}$ value for the isolated *Chaetoceros* is 9.0 ± 0.6‰ (Fig. 4a). The relative abundance of CRS ranges from 79-95%, with relative surface area ($\%CRS_{SA}$) ranging between 74-89% of total diatom surface area (Table 2).

Table 2: Data from ODP Core 1098B-5H-7 deglacial sediments

Sample	Depth (cm)	$\delta^{15}N_{DB\text{-}bulk}$ (‰)	$\delta^{15}N_{DB\text{-}Ch}$ (‰)	%CRS (surface area)	%CRS (count)	CRS/*Ch.* (%)
1	12-14.5	9.3	9.2	89	95	96
2	15-18	9.8	9.5	83	91	93
3	25.5-27	10.3	9.1	78	87	91
4	27.5-31	9.2	9.3	83	85	87
5	44.5-47	8.9	7.9	74	83	86
6	63.5-65.5	8.9	8.9	77	79	84

Note. $\delta^{15}N_{DB\text{-}bulk}$ describes the measurements from the entire <63 μm diatom community and $\delta^{15}N_{DB\text{-}Ch}$ describes the measurements from isolated *Chaetoceros*.

4 Discussion

4.1 Accounting for differences in culture and sediment $\delta^{15}N_{DB}$ measurements

Both culture experiments and sedimentary data suggest that CRS are characterized by low $\delta^{15}N_{DB}$ values relative to vegetative *Chaetoceros* and to other diatoms, but our measurements of CRS-specific $\delta^{15}N_{DB}$ range from approximately -1‰ in culture to approximately 8‰ in sediments. Since differences in CRS-specific $\delta^{15}N_{DB}$ absolute values are expected due to variation in source $\delta^{15}N_{NO3}$, we focus our discussion on the relationship between $\delta^{15}N_{DB}$ values in CRS and non-CRS diatoms ($\Delta\delta^{15}N_{CRS}$).

https://doi.org/10.5194/egusphere-2023-2564
Preprint. Discussion started: 16 November 2023
© Author(s) 2023. CC BY 4.0 License.

4.2 Quantitative $\delta^{15}N_{DB}$ differences between CRS and non-CRS diatoms

The difference between cultured vegetative *Chaetoceros* and CRS $\delta^{15}N_{DB}$ values is quantified in two ways: 1) using data from experiment 3 and 2) using data from all experiments. Firstly, the $\delta^{15}N_{DB}$ values of two successfully isolated CRS samples are on average 7.7 ± 0.5‰ lower than their vegetative counterparts (Fig. 3). Prior to calculating this difference for carboy 2, the vegetative $\delta^{15}N_{DB}$ measurement was corrected from 4.6 ± 0.2‰ to 4.9 ± 0.5‰, to account for the 4% of cells that had sporulated. To do so, we assume a $\delta^{15}N_{DB}$ value of -2.8 ± 0.4‰ for the CRS based the CRS-specific $\delta^{15}N_{DB}$ measurement from carboy 2. In the second calculation, where all experimental data are included, a mass balance calculation using average vegetative sample and mixed sample $\delta^{15}N_{DB}$ values, and assuming that 17% of cells are resting spores, yields a difference of 6.3 ± 3.7‰. Together, these independent calculations suggest that CRS record $\delta^{15}N_{DB}$ values 7.0 ± 2.6‰ lower than vegetative *Chaetoceros*.

To compare differences in assemblage-specific $\delta^{15}N_{DB}$ values in sediment, we must account for varying surface area contributions between samples. Using a simple mass balance calculation (Eq. 1), we find that the isolated *Chaetoceros* samples have a $\delta^{15}N_{DB}$ value 1.9 ± 2.3‰ lower than non-*Chaetoceros* diatoms ($\delta^{15}N_{DB\text{-}other}$).

$$\delta^{15}N_{DB-bulk} = \delta^{15}N_{DB-Ch} \times \%CRS_{SA} + \delta^{15}N_{DB-other} \times (1 - \%CRS_{SA}) \quad (1)$$

However, the $\delta^{15}N_{DB\text{-}Ch}$ measurements are influenced by vegetative *Chaetoceros* present in the isolated samples. To correct for this, we assume that the proportion of CRS to all *Chaetoceros* valves (CRS/*Ch.*) is consistent between the bulk community and the isolated samples. We also assume that vegetative *Chaetoceros* and CRS are the same size and thus have a consistent conversion between relative count and relative surface area. Finally, using culture data, we assume that vegetative $\delta^{15}N_{DB}$ values are 7.0‰ higher than CRS $\delta^{15}N_{DB}$ values. We calculate the $\delta^{15}N_{DB}$ value for only CRS ($\delta^{15}N_{DB\text{-}CRS}$) using Eq. 2:

$$\delta^{15}N_{DB-Ch} = \delta^{15}N_{DB-CRS} \times \left(\frac{CRS}{Ch.}\right) + (\delta^{15}N_{DB-CRS} + 7.0‰) \times \left(1 - \frac{CRS}{Ch.}\right) \quad (2)$$

Next, we use our calculated $\delta^{15}N_{DB\text{-}CRS}$ values to determine $\delta^{15}N_{DB\text{-}other}$ with Eq. 3:

$$\delta^{15}N_{DB-bulk} = \delta^{15}N_{DB-CRS} \times \%CRS_{SA} + \delta^{15}N_{DB-other} \times (1 - \%CRS_{SA}) \quad (3)$$

Between the 6 samples, average $\delta^{15}N_{DB\text{-}CRS}$ is 8.2 ± 0.8‰ and average $\delta^{15}N_{DB\text{-}other}$ is 13.9 ± 1.6‰, resulting in a $\Delta\delta^{15}N_{CRS}$ value of 5.6 ± 1.9‰ (Fig. 4b).

https://doi.org/10.5194/egusphere-2023-2564
Preprint. Discussion started: 16 November 2023
© Author(s) 2023. CC BY 4.0 License.

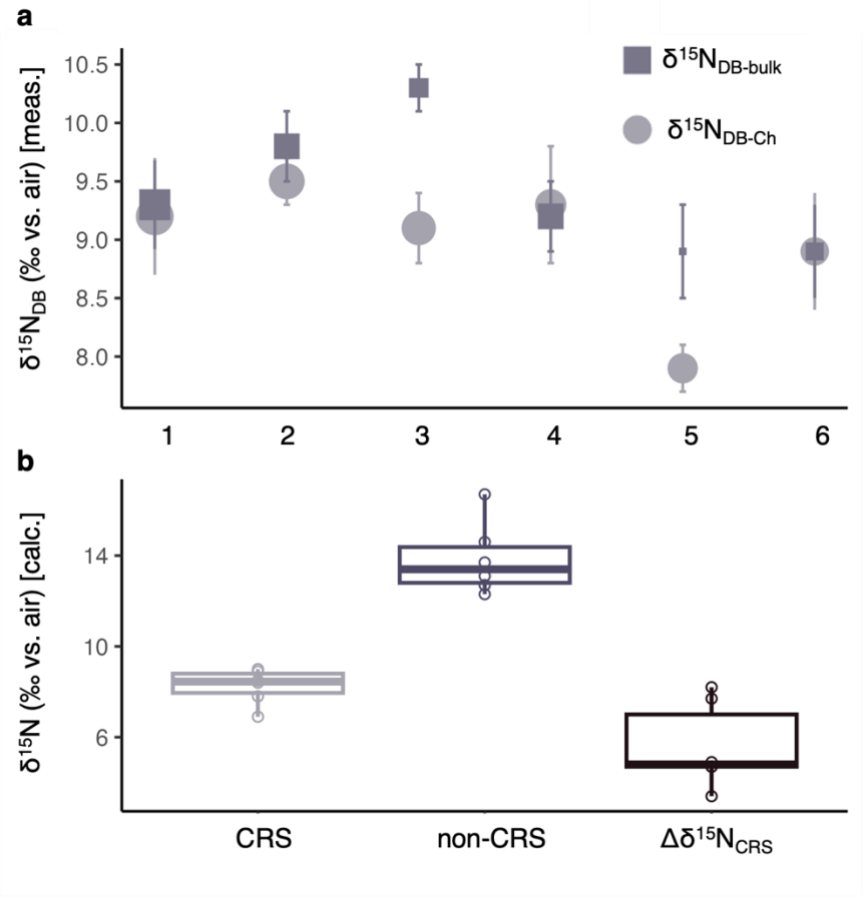

335 **Figure 4: $\delta^{15}N_{DB}$ measurements and calculated assemblage-specific $\delta^{15}N_{DB}$ values from ODP Site 1098 sediments. Panel (a) shows $\delta^{15}N_{DB}$ measured from the entire <63 µm diatom community ($\delta^{15}N_{DB\text{-}bulk}$; squares) and from isolated *Chaetoceros* ($\delta^{15}N_{DB\text{-}Ch}$; circles). $\delta^{15}N_{DB\text{-}bulk}$ point markers are scaled to CRS surface area contribution (%CRS_{SA}) and $\delta^{15}N_{DB\text{-}Ch}$ point markers are scaled to the proportion of CRS in the isolated *Chaetoceros* sample (CRS/*Ch.*). Panel (b) shows boxplots of calculated CRS-specific $\delta^{15}N_{DB}$ values ($\delta^{15}N_{DB\text{-}CRS}$), non-CRS $\delta^{15}N_{DB}$ values ($\delta^{15}N_{DB\text{-}other}$), and the difference between them ($\Delta\delta^{15}N_{CRS}$).**

340 **4.3 Vegetative *Chaetoceros* and CRS ε_{DB}**

Since $\delta^{15}N_{DB}$ values are influenced by fractionation during N incorporation into frustules, ε_{DB} ($\delta^{15}N_{biomass}$ - $\delta^{15}N_{DB}$) values are essential for relating measured $\delta^{15}N_{DB}$ to past surface nutrient conditions (Horn et al., 2011a; Jones et al., 2022). Excluding the sample from carboy 2 that contains CRS, the calculated ε_{DB} value for vegetative *Chaetoceros* in experiment 3 is 0.4 ± 1.4‰, while the calculated ε_{DB} value for vegetative *Chaetoceros* across all experiments is -1.5 ± 2.6‰. In contrast to
345 vegetative *Chaetoceros*, CRS are characterized by an anomalously high ε_{DB} value of 8.0 ± 2.7‰ (Fig. 3).

While Horn et al. (2011a) found ε_{DB} values up to 11.2‰ in monospecific diatom cultures, additional culture studies (Jones et al., 2022) and fieldwork (Morales et al., 2014; Robinson et al., 2020) show consistently negative ε_{DB} values for diatom

https://doi.org/10.5194/egusphere-2023-2564
Preprint. Discussion started: 16 November 2023
© Author(s) 2023. CC BY 4.0 License.

communities. Our calculated average ε_{DB} value (-1.5 ± 2.6‰) for vegetative *Chaetoceros* is consistent with modern field observations (-3.2 ± 1.5‰; Robinson et al., 2020) and experimental results (-4.8± 1.5‰; Jones et al., 2022).

4.4 Reasons for low CRS $\delta^{15}N_{DB}$ values

Our results are surprising given that CRS form under nutrient depleted conditions, when one would expect high $\delta^{15}N_{DB}$ values reflective of high $\delta^{15}N_{NO3}$. Nevertheless, $\Delta\delta^{15}N_{CRS}$ values are comparable between cultures (7.0 ± 2.6‰) and sediment (5.6 ± 1.9‰). We identify three possible explanations for why CRS record low $\delta^{15}N_{DB}$ values relative to vegetative *Chaetoceros* and to other diatoms: ammonium assimilation, silicification, and internal N fractionation during sporulation.

4.4.1 Reduced N assimilation

Lower $\delta^{15}N_{biomass}$ values observed after resting spore formation in the experiment suggest assimilation of isotopically light N, likely ammonium or other bioavailable reduced N. Observed increases in reduced N concentration throughout the experiment are likely due to remineralization by bacteria since the cultures are not axenic, while decreases are due to consumption by both diatoms and bacteria. Although bacterial nutrient consumption is not quantified, we assume that it minimally influences interpretations because the majority of nutrient N is nitrate consumed by diatoms.

Southern Ocean field observations from late in the diatom growing season suggest that assimilation of regenerated ammonium results in low particulate and diatom-bound $\delta^{15}N$ values (Robinson et al., 2020). Ammonium concentrations measured throughout the culture experiment suggest that ammonium, either regenerated or preexisting in culture media, is consumed prior to and during CRS formation (Fig. 2). Given consistently low $\delta^{15}N$ values for total reduced N, ammonium assimilation could lead to lower $\delta^{15}N_{DB}$ values in CRS.

While ammonium, or another form of bioavailable reduced N such as urea, likely contributed to lower $\delta^{15}N_{DB}$ values, it does not fully account for the large difference between CRS and vegetative cells. Conservatively estimating that all reduced N consumed has a $\delta^{15}N$ value of -2‰, it is not possible for assimilation alone to explain why measured CRS $\delta^{15}N_{DB}$ values are 7.0 ± 2.6‰ lower than that of vegetative *Chaetoceros* (see Supplement S2).

4.4.2 Silicification

Although no research into CRS silicification has presently been published, past work on silicification using the model species *Thalassiosira pseudonana* shows that genes involved in silicification are upregulated at times when frustule structures are not being made (Tesson et al., 2017; Kotzsch et al., 2017). The implication that proteins are synthesized before they are needed suggests that the N-containing structures necessary for sporulation could be synthesized prior to nutrient depletion, when ^{14}N is more abundant. If this is the case, the N bound within CRS could have inherited its low $\delta^{15}N$ value from dissolved nutrients early in the growing season.

https://doi.org/10.5194/egusphere-2023-2564
Preprint. Discussion started: 16 November 2023
© Author(s) 2023. CC BY 4.0 License.

Previous culture work suggests an association between silicification and ε_{DB}. Jones (2020) found a significant relationship between Si:N uptake and ε_{DB}, which could potentially bias $\delta^{15}N_{DB}$ towards lower values for heavily silicified diatoms. Since CRS are more heavily silicified than vegetative *Chaetoceros*, silicification could be an important driver of low $\delta^{15}N_{DB}$ in CRS. Still, further research is necessary to characterize the Si:N relationship in different species and to identify the mechanism behind this relationship.

4.4.3 Internal fractionation

With similar $\delta^{15}N_{biomass}$ values between vegetative *Chaetoceros* and CRS, low $\delta^{15}N_{DB}$ values in CRS consequently lead to high calculated ε_{DB} values. Although our CRS-specific ε_{DB} calculations are affected by biomass accumulated from vegetative *Chaetoceros*, the large difference between $\delta^{15}N_{biomass}$ and CRS $\delta^{15}N_{DB}$ points to internal fractionation processes that greatly favor incorporation of ^{14}N into resting spore frustules. This internal fractionation may be related to available nutrients and silicification. While our work does not provide an answer as to why CRS display strong internal fractionation, our data show a clear trend of CRS recording low $\delta^{15}N_{DB}$ values that warrants future investigation.

4.5 Paleoceanographic implications

Since CRS can comprise a significant proportion of sedimentary diatom assemblages in the Southern Ocean (Crosta et al., 1997; Armand et al., 2005; Esper et al., 2010; Zielinski and Gersonde, 1997), their unique N isotopic signature must be considered when applying the $\delta^{15}N_{DB}$ proxy to paleoceanographic research, particularly quantitative reconstructions (e.g., Kemeny et al., 2018). A pertinent case study is that of glacial-interglacial cycles, wherein $\delta^{15}N_{DB}$ values tend to increase during glacial periods (Robinson et al., 2004, 2005; Studer et al., 2015; Ai et al., 2020) and CRS relative abundance is expected to increase due to increased sea ice extent (Abelmann et al., 2006).

Diatom assemblage data and $\delta^{15}N_{DB}$ measurements spanning at least one glacial-interglacial cycle are available from sediment cores TN057-13-PC4 and MD11-3353, which are respectively located in the AZ of the Atlantic sector and the Polar Front Zone of the Indian sector of the Southern Ocean (Fig. 1). The $\delta^{15}N_{DB}$ record from TN057-13-PC4, which spans ~23 ka to present, is unique in that interglacial values are higher than glacial values (Horn et al., 2011b). The CRS relative abundance is consistently below 10% during the Holocene and reaches a maximum of ~40% during the last glacial (Nielsen, 2004; Fig. 5a). In the 150-kyr MD11-3353 record, glacial $\delta^{15}N_{DB}$ values are ~4‰ lower than interglacial values (Ai et al., 2020) and CRS relative abundance peaks around 30% following the most recent deglaciation ~12 ka (Civel-Mazens et al., 2021; Fig. 5b). A smaller CRS peak occurs ~130 ka.

To assess how diatom assemblage impacts $\delta^{15}N_{DB}$ records on glacial-interglacial timescales, we first calculate average relative abundance of relevant diatoms during glacial versus interglacial periods. For TN057-13-PC4, we define the

https://doi.org/10.5194/egusphere-2023-2564
Preprint. Discussion started: 16 November 2023
© Author(s) 2023. CC BY 4.0 License.

Holocene (11.7 ka-present) as interglacial and 23-18 ka as glacial. For the longer record from MD11-3353, we define glacial and interglacial periods based on the marine isotope stages delineated by Lisiecki & Raymo (2005). For both cores, we focus on four diatom groups: CRS, *Eucampia antarctica*, *Fragilariopsis kerguelensis*, and *Thalassiosira lentiginosa* due to their high relative abundances and shifting biogeography across glacial-interglacial timescales (Jacot Des Combes et al., 2008).

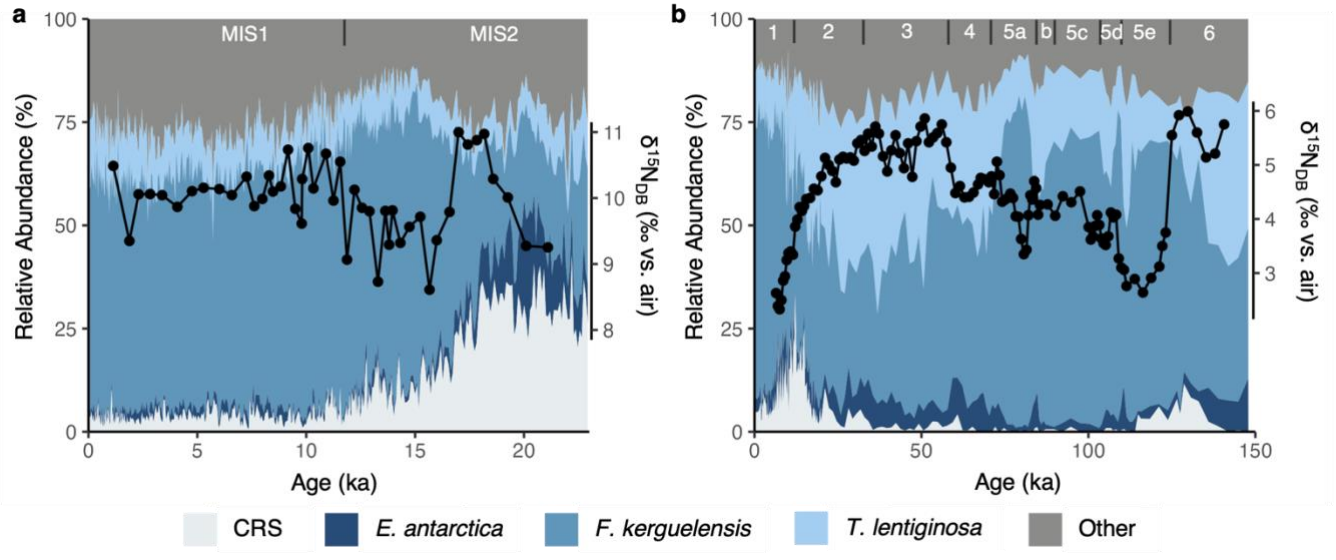

Figure 5: $\delta^{15}N_{DB}$ records and diatom assemblage data from sediment cores TN057-13-PC4 (a) and MD11-3353 (b). TN057-13-PC4 $\delta^{15}N_{DB}$ data from Horn et al. (2011b) and diatom data from Nielsen (2004). MD11-3353 $\delta^{15}N_{DB}$ data from Ai et al. (2020) and diatom data from Civel-Mazens et al. (2021).

Following the methodology of Horn et al. (2011a), we calculate expected differences in glacial-interglacial $\delta^{15}N_{DB}$ values due to changes in diatom assemblage with a mass balance equation including species-specific ε_{DB} values and diatom species relative abundances. While different $\delta^{15}N_{DB}$ values across glacial-interglacial cycles reflect changes in nutrient utilization, the relationship between $\delta^{15}N_{DB}$ and $\delta^{15}N_{biomass}$, or ε_{DB}, should remain consistent regardless of nutrient utilization. Therefore, changes in community ε_{DB} over time reflect only assemblage-driven effects. We assign the published ε_{DB} value of -3.2‰ for diatom communities in the AZ (Robinson et al., 2020) to all diatoms except CRS. For CRS, we constrain our ε_{DB} value using sedimentary $\delta^{15}N_{DB}$ data. The sedimentary data are preferred over the culture data because they eliminate any bias introduced from reduced N assimilation in the culture experiments. Since the sedimentary data suggest that CRS record $\delta^{15}N_{DB}$ values 5.6 ± 1.9‰ lower than non-CRS diatoms, we use an ε_{DB} value of 2.4‰ for CRS in our calculation (-3.2‰ + 5.6‰, assuming constant $\delta^{15}N_{biomass}$).

Using these ε_{DB} parameters along with relative abundance data, we find that the calculated glacial ε_{DB} value is 1.6‰ lower than the calculated interglacial ε_{DB} value in TN057-13-PC4, meaning that glacial $\delta^{15}N_{DB}$ values are expected to be 1.6‰ lower than interglacial $\delta^{15}N_{DB}$ values due to changes in diatom assemblage alone. CRS relative abundance in MD11-3353 is

https://doi.org/10.5194/egusphere-2023-2564
Preprint. Discussion started: 16 November 2023
© Author(s) 2023. CC BY 4.0 License.

only slightly greater during glacial periods, resulting in a glacial ε_{DB} value 0.1‰ lower than that of interglacial periods (Table 3).

Table 3: Mass balance calculation of estimated community ε_{DB} values in glacial versus interglacial sediments

		ε_{DB}* (‰)	Avg. SA (μm^2)†	RA (%)	SA (%)‡
		TN057-13-PC4			
Glacial	CRS	2.4	170	32	5
	E. antarctica	-3.2	2246	15	32
	F. kerguelensis	-3.2	1081	24	24
	T. lentiginosa	-3.2	4418	7	29
	Other diatoms	-3.2		22	10
		Estimated community ε_{DB} (‰)		-1.4	-2.9
Interglacial	CRS	2.4	170	4	1
	E. antarctica	-3.2	2246	2	3
	F. kerguelensis	-3.2	1081	57	50
	T. lentiginosa	-3.2	4418	10	36
	Other diatoms	-3.2		27	10
		Estimated community ε_{DB} (‰)		-3.0	-3.2
		Glacial-interglacial ε_{DB} difference (‰)		**1.6**	**0.3**
		MD11-3353			
Glacial	CRS	2.4	170	7	1
	E. antarctica	-3.2	2246	5	5
	F. kerguelensis	-3.2	1081	39	20
	T. lentiginosa	-3.2	4418	30	64
	Other diatoms	-3.2		19	10
		Estimated community ε_{DB}		-2.8	-3.2
Interglacial	CRS	2.4	170	5	1
	E. antarctica	-3.2	2246	5	6
	F. kerguelensis	-3.2	1081	56	35
	T. lentiginosa	-3.2	4418	19	48
	Other diatoms	-3.2		15	10
		Estimated community ε_{DB}		-2.9	-3.2
		Glacial-interglacial ε_{DB} difference (‰)		**0.1**	**0**

https://doi.org/10.5194/egusphere-2023-2564
Preprint. Discussion started: 16 November 2023
© Author(s) 2023. CC BY 4.0 License.

Note. Community ε_{DB} estimates are calculated using both diatom relative abundance (RA) and diatom surface area (SA) contribution.
*non-CRS ε_{DB} estimate from Robinson et al. (2020).
†Average surface area calculated with parameters reported in Leblanc et al. (2012)
‡Percent SA = 100 * (RA * SA avg) / Total SA. In all cases, we assume that other diatoms comprise 10% of total diatom SA.

Because relative surface area is a more accurate measure of CRS contribution to the $\delta^{15}N_{DB}$ signal than relative abundance, we estimate the average two-dimensional surface area and relative surface area contribution for each diatom group using biometric data from Leblanc et al. (2012) to recalculate expected glacial versus interglacial community ε_{DB} values. Three-dimensional surface area or biovolume likely provide more accurate estimates of N contribution but are much more difficult to quantitatively measure in sediments since only two axes are measurable on microscope slides. Calculations using estimates of biovolume and three-dimensional surface area were also performed and did not change interpretations (see Supplement S3). Species-specific Si:N data would provide the most accurate constraint on individual contributions to the $\delta^{15}N_{DB}$ signal, but these data are not currently available. We therefore present results calculated with two-dimensional surface area.

Our calculation reveals that differences in glacial versus interglacial community ε_{DB}, and thus expected assemblage-related differences in glacial versus interglacial $\delta^{15}N_{DB}$ values, are reduced to 0.3‰ and 0‰ in TN057-13-PC4 and MD11-3353, respectively, when considering surface area (Table 3). Given that typical measurement precision is ~0.3‰, the theoretical assemblage-specific effects on $\delta^{15}N_{DB}$ records are negligible. Although CRS relative abundance increases by nearly 30% in TN057-13-PC4 during the glacial period, CRS relative contribution to total diatom surface area increases by only about 4% due to the small size of CRS compared to other diatoms such as *T. lentiginosa* (Table 3).

While $\delta^{15}N_{DB}$ records are negatively skewed by increased resting spore relative abundance, the expected bias across glacial-interglacial cycles in these examples, calculated with surface area, is not significant and does not change interpretations of nutrient utilization across glacial-interglacial cycles. Larger fluctuations in CRS relative abundance and, importantly, changes in surface area contribution exceeding 5% could lead to confounding differences in $\delta^{15}N_{DB}$ values over time. Considering glacial-interglacial shifts in diatom assemblage is important because increased CRS abundance during glacial periods could potentially skew $\delta^{15}N_{DB}$ measurements towards lower values and therefore lead to underestimates of the biological pump's role in lowering glacial atmospheric CO_2.

5 Conclusions

Results from our culture experiments and sedimentary measurements show that CRS record low $\delta^{15}N_{DB}$ values relative to vegetative *Chaetoceros* and other diatoms. This is surprising because CRS form when nutrients are depleted and

https://doi.org/10.5194/egusphere-2023-2564
Preprint. Discussion started: 16 November 2023
© Author(s) 2023. CC BY 4.0 License.

consequently when $\delta^{15}N_{NO3}$ is elevated. Low $\delta^{15}N_{DB}$ values in CRS are tentatively attributed to ammonium assimilation, heavy silicification, and strong internal fractionation processes, but additional research into CRS formation and silicification is necessary to provide further insights into such processes.

N isotopic data from culture experiments and sediment, paired with diatom assemblage data, suggest that increased CRS abundance in open ocean sediments does not significantly bias $\delta^{15}N_{DB}$ records across glacial-interglacial cycles. However, lower $\delta^{15}N_{DB}$ values in CRS may be relevant to $\delta^{15}N_{DB}$ records generated in coastal regions, such as the Antarctic Peninsula, where CRS are especially abundant. Estimates of $\delta^{15}N_{DB}$ biases over time due to changing diatom communities can be further honed with similar studies of relevant species, such as *E. antarctica*. Ultimately, our work highlights the importance of considering diatom assemblage changes throughout sedimentary $\delta^{15}N_{DB}$ records, especially when such records are applied for quantitative paleo reconstructions.

Data availability

Data are available in the Supplement and in the U.S. Antarctic Program Data Center (https://doi.org/10.15784/601727; https://doi.org/10.15784/601720; https://doi.org/10.15784/601723).

Author contribution

IAD, RSR, and RPK designed the culture experiments. NR provided PS119 sediment samples and IWB performed18S rDNA sequencing. Culture experiments, sample measurement, and sediment analyses were performed by IAD. XC provided diatom assemblage data from TN057-13-PC4 and MD11-3353. All authors contributed to interpreting data. IAD prepared the manuscript with contributions from all co-authors.

Competing interests

The authors declare that they have no conflict of interest.

Acknowledgements

This work was supported by NSF OPP award #1744871 to R.S.R. N.R. received funding from NSF OCE award #1847509. Thanks to E. Baker and D. Outram of the Marine Science Research Facility for assistance with facilities and instrumentation necessary to maintain laboratory cultures. Thanks to S. Setta for assistance with isolating diatoms and to C. Gelfman, S. Lerch, and T. Rynearson for taking samples during experiment 2.

https://doi.org/10.5194/egusphere-2023-2564
Preprint. Discussion started: 16 November 2023
© Author(s) 2023. CC BY 4.0 License.

References

Abelmann, A., Gersonde, R., Cortese, G., Kuhn, G., and Smetacek, V.: Extensive phytoplankton blooms in the Atlantic sector of the glacial Southern Ocean, Paleoceanography, 21, 1013, https://doi.org/10.1029/2005PA001199, 2006.

Ai, X. E., Studer, A. S., Sigman, D. M., Martínez-García, A., Fripiat, F., Thöle, L. M., Michel, E., Gottschalk, J., Arnold, L., Moretti, S., Schmitt, M., Oleynik, S., Jaccard, S. L., and Haug, G. H.: Southern Ocean upwelling, Earth's obliquity, and glacial-interglacial atmospheric CO 2 change, Science (1979), 370, 1348–1352, 2020.

Altabet, M. A. and Francois, R.: Sedimentary nitrogen isotopic ratio as a recorder for surface ocean nitrate utilization, Global Biogeochem Cycles, 8, 103–116, https://doi.org/10.1029/93GB03396, 1994.

Armand, L. K., Crosta, X., Romero, O., and Pichon, J. J.: The biogeography of major diatom taxa in Southern Ocean sediments: 1. Sea ice related species, Palaeogeogr Palaeoclimatol Palaeoecol, 223, 93–126, https://doi.org/10.1016/J.PALAEO.2005.02.015, 2005.

Bishop, I. W., Anderson, S. I., Collins, S., and Rynearson, T. A.: Thermal trait variation may buffer Southern Ocean phytoplankton from anthropogenic warming, Glob Chang Biol, 28, 5755–5767, https://doi.org/10.1111/GCB.16329, 2022.

Bohrmann, G.: The expedition PS119 of the research vessel POLARSTERN to Eastern Scotia Sea in 2019, Bremerhaven, Germany, 2019.

Braman, R. S. and Hendrix, S. A.: Nanogram Nitrite and Nitrate Determination in Environmental and Biological Materials by Vanadium(III) Reduction with Chemiluminescence Detection, Anal Chem, 61, 2715–2718, 1989.

Civel-Mazens, M., Crosta, X., Cortese, G., Michel, E., Mazaud, A., Ther, O., Ikehara, M., and Itaki, T.: Impact of the Agulhas Return Current on the oceanography of the Kerguelen Plateau region, Southern Ocean, over the last 40 kyrs, Quat Sci Rev, 251, 106711, 2021.

Crosta, X. and Koç, N.: Chapter Eight Diatoms: From Micropaleontology to Isotope Geochemistry, Developments in Marine Geology, 1, 327–369, https://doi.org/10.1016/S1572-5480(07)01013-5, 2007.

Crosta, X., Pichon, J.-J., and Labracherie, M.: Distribution of *Chaetoceros* resting spores in modem peri-Antarctic sediments, Marine Micropaleontology, 283–299 pp., 1997.

Denis, D., Crosta, X., Zaragosi, S., Romero, O., Martin, B., and Mas, V.: Seasonal and subseasonal climate changes recorded in laminated diatom ooze sediments, Adélie Land, East Antarctica, Holocene, 16, 1137–1147, https://doi.org/10.1177/0959683606069414, 2006.

Egan, K. E., Rickaby, R. E. M., Leng, M. J., Hendry, K. R., Hermoso, M., Sloane, H. J., Bostock, H., and Halliday, A. N.: Diatom silicon isotopes as a proxy for silicic acid utilisation: A Southern Ocean core top calibration, Geochim Cosmochim Acta, 96, 174–192, https://doi.org/10.1016/J.GCA.2012.08.002, 2012.

Esper, O., Gersonde, R., and Kadagies, N.: Diatom distribution in southeastern Pacific surface sediments and their relationship to modern environmental variables, Palaeogeogr Palaeoclimatol Palaeoecol, 287, 1–27, https://doi.org/10.1016/J.PALAEO.2009.12.006, 2010.

https://doi.org/10.5194/egusphere-2023-2564
Preprint. Discussion started: 16 November 2023
© Author(s) 2023. CC BY 4.0 License.

François, R., Altabett, M. A., Yu, E. F., Sigman, D. M., Bacon, M. P., Frank, M., Bohrmann, G., Bareille, G., and Labeyrie, L. D.: Water column stratification in the Southern Ocean contributed to the lowering of glacial atmospheric CO2, Nature, 389, 929–935, https://doi.org/10.1038/40073, 1997.

French, F. W. and Hargraves, P. E.: Spore Formation in the Life Cycles of the Diatoms *Chaetoceros diadema* and *Leptocylindrus danicus*, J Phycol, 21, 477–483, https://doi.org/10.1111/J.0022-3646.1985.00477.X, 1985.

Gersonde, R., Crosta, X., Abelmann, A., and Armand, L.: Sea-surface temperature and sea ice distribution of the Southern Ocean at the EPILOG Last Glacial Maximum—a circum-Antarctic view based on siliceous microfossil records, Quat Sci Rev, 24, 869–896, https://doi.org/10.1016/J.QUASCIREV.2004.07.015, 2005.

Guillard, R. R. L.: Culture of phytoplankton for feeding marine invertebrates, in: Culture of marine invertebrate animals, edited by: Smith, W. L. and Chanley, M. H., Springer, 29–60, 1975.

Hasle, G. R. and Syvertsen, E. E.: Identifying Marine Phytoplankton, edited by: Tomas, C. R., Academic Press, San Diego, 1997.

Hildebrand, M., Lerch, S. J. L., and Shrestha, R. P.: Understanding diatom cell wall silicification-moving forward, Front Mar Sci, 5, 125, https://doi.org/10.3389/FMARS.2018.00125/BIBTEX, 2018.

Holmes, R. M., Aminot, A., Kérouel, R., Hooker, B. A., and Peterson, B. J.: A simple and precise method for measuring ammonium in marine and freshwater ecosystems, Canadian Journal of Fish and Aquatic Sciences, 56, 1801–1808, https://doi.org/10.1139/F99-128, 1999.

Horn, M. G., Robinson, R. S., Rynearson, T. A., and Sigman, D. M.: Nitrogen isotopic relationship between diatom-bound and bulk organic matter of cultured polar diatoms, Paleoceanography, 26, https://doi.org/10.1029/2010PA002080, 2011a.

Horn, M. G., Beucher, C. P., Robinson, R. S., and Brzezinski, M. A.: Southern Ocean nitrogen and silicon dynamics during the last deglaciation, Earth Planet Sci Lett, 310, 334–339, https://doi.org/10.1016/j.epsl.2011.08.016, 2011b.

Jacot Des Combes, H. J., Esper, O., De La Rocha, C. L., Abelmann, A., Gersonde, R., Yam, R., and Shemesh, A.: Diatom δ13C, δ15N, and C/N since the Last Glacial Maximum in the Southern Ocean: Potential impact of Species Composition, Paleoceanography, 23, https://doi.org/10.1029/2008PA001589, 2008.

Jones, C.: Raise your glass: A culture evaluation of diatoms as archives of past nutrient consumption, Ph.D. thesis, University of Rhode Island, 2020.

Jones, C. A., Closset, I., Riesselman, C. R., Kelly, R. P., Brzezinski, M. A., and Robinson, R. S.: New Constraints on Assemblage-Driven Variation in the Relationship Amongst Diatom-Bound, Biomass, and Nitrate Nitrogen Isotope Values, Paleoceanogr Paleoclimatol, 37, https://doi.org/10.1029/2022pa004428, 2022.

Kemeny, P. C., Kast, E. R., Hain, M. P., Fawcett, S. E., Fripiat, F., Studer, A. S., Martínez-García, A., Haug, G. H., and Sigman, D. M.: A Seasonal Model of Nitrogen Isotopes in the Ice Age Antarctic Zone: Support for Weakening of the Southern Ocean Upper Overturning Cell, Paleoceanogr Paleoclimatol, 33, 1453–1471, https://doi.org/10.1029/2018PA003478, 2018.

https://doi.org/10.5194/egusphere-2023-2564
Preprint. Discussion started: 16 November 2023
© Author(s) 2023. CC BY 4.0 License.

Knapp, A. N., Sigman, D. M., and Lipschultz, F.: N isotopic composition of dissolved organic nitrogen and nitrate at the Bermuda Atlantic Time-series study site, Global Biogeochem Cycles, 19, 1–15, https://doi.org/10.1029/2004GB002320, 2005.

Knox, F. and McElroy, M. B.: Changes in atmospheric CO_2 influence of the marine biota at high latitude, J. Geophys. Res., 89, 4629–4637, https://doi.org/10.1029/jd089id03p04629, 1984.

Kotzsch, A., Gröger, P., Pawolski, D., Bomans, P. H. H., Sommerdijk, N. A. J. M., Schlierf, M., and Kröger, N.: Silicanin-1 is a conserved diatom membrane protein involved in silica biomineralization, BMC Biol, 15, https://doi.org/10.1186/S12915-017-0400-8, 2017.

Kröger, N., Deutzmann, R., and Sumper, M.: Polycationic peptides from diatom biosilica that direct silica nanosphere formation, Science (1979), 286, 1129–1132, https://doi.org/10.1126/SCIENCE.286.5442.1129, 1999.

Kröger, N., Deutzmann, R., Bergsdorf, C., and Sumper, M.: Species-specific polyamines from diatoms control silica morphology, Proc Natl Acad Sci U S A, 97, 14133–14138, https://doi.org/10.1073/PNAS.260496497, 2000.

Kuwata, A., Hama, T., and Takahashi, M.: Ecophysiological characterization of two life forms, resting spores and resting cells, of a marine planktonic diatom, *Chaetoceros pseudocurvisetus*, formed under nutrient depletion, Mar Ecol Prog Ser, 102, 245–255, 1993.

Leblanc, K., Arístegui, J., Armand, L., Assmy, P., Beker, B., Bode, A., Breton, E., Cornet, V., Gibson, J., Gosselin, M.-P., Kopczynska, E., Marshall, H., Peloquin, J., Piontkovski, S., Poulton, A. J., Qú Eguiner, B., Schiebel, R., Shipe, R., Stefels, J., Van Leeuwe, M. A., Varela, M., Widdicombe, C., and Yallop, M.: A global diatom database - abundance, biovolume and biomass in the world ocean, Earth Syst. Sci. Data Discuss, 5, 147–185, https://doi.org/10.5194/essdd-5-147-2012, 2012.

Leventer, A.: Sediment trap diatom assemblages from the northern Antarctic Peninsula region, Deep Sea Research Part A. Oceanographic Research Papers, 38, 1127–1143, https://doi.org/10.1016/0198-0149(91)90099-2, 1991.

Lisiecki, L. E. and Raymo, M. E.: A Pliocene-Pleistocene stack of 57 globally distributed benthic δ18O records, Paleoceanography, 20, 1–17, https://doi.org/10.1029/2004PA001071, 2005.

Maddison, E. J., Pike, J., Leventer, A., and Domack, E. W.: Deglacial seasonal and sub-seasonal diatom record from Palmer Deep, Antarctica, J Quat Sci, 20, 435–446, https://doi.org/10.1002/JQS.947, 2005.

Martin, J. H.: Glacial-interglacial CO2 change: The Iron Hypothesis, Paleoceanography, 5, 1–13, https://doi.org/10.1029/PA005I001P00001, 1990.

Martínez-García, A., Sigman, D. M., Ren, H., Anderson, R. F., Straub, M., Hodell, D. A., Jaccard, S. L., Eglinton, T. I., and Haug, G. H.: Iron fertilization of the subantarctic ocean during the last ice age, Science (1979), 343, 1347–1350, https://doi.org/10.1126/SCIENCE.1246848/SUPPL_FILE/MARTINEZ-GARCIA.SM.PDF, 2014.

Mitchell, B. G., Brody, E. A., Holm-Hansen, O., McClain, C., and Bishop, J.: Light limitation of phytoplankton biomass and macronutrient utilization in the Southern Ocean, Limnol Oceanogr, 36, 1662–1677, https://doi.org/10.4319/LO.1991.36.8.1662, 1991.

https://doi.org/10.5194/egusphere-2023-2564
Preprint. Discussion started: 16 November 2023
© Author(s) 2023. CC BY 4.0 License.

Morales, L. v., Sigman, D. M., Horn, M. G., and Robinson, R. S.: Cleaning methods for the isotopic determination of diatom-bound nitrogen in non-fossil diatom frustules, Limnol Oceanogr Methods, 11, 101–112, https://doi.org/10.4319/lom.2013.11.101, 2013.

Morales, L. v., Granger, J., Chang, B. X., Prokopenko, M. G., Plessen, B., Gradinger, R., and Sigman, D. M.: Elevated 15N/14N in particulate organic matter, zooplankton, and diatom frustule-bound nitrogen in the ice-covered water column of the Bering Sea eastern shelf, Deep Sea Research Part II: Topical Studies in Oceanography, 109, 100–111, https://doi.org/10.1016/J.DSR2.2014.05.008, 2014.

Nielsen, S.: Southern Ocean climate variability, Ph.D. thesis, University of Tromso and Norwegian Polar Institute, Tromso, Norway, 2004.

Oku, O. and Kamatani, A.: Resting spore formation of the marine planktonic diatom *Chaetoceros anastomosans* induced by high salinity and nitrogen depletion, Mar Biol, 127, 515–520, 1997.

Orsi, A., Whitworth III, T., and Nowlin Jr., W.: On the meridional extent and fronts of the Antarctic Circumpolar Current, Deep Sea Research Part I: Oceanographic Research Papers, 42, 641–673, 1995.

Pelusi, A., Santelia, M. E., Benevenuto, G., Godhe, A., and Montresor, M.: The diatom *Chaetoceros socialis*: spore formation and preservation, Eur J Phycol, 55, 1–10, https://doi.org/10.1080/09670262.2019.1632935, 2020.

Pichon, J. J., Bareille, G., Labracherie, M., Labeyrie, L. D., Baudrimont, A., and Turon, J. L.: Quantification of the Biogenic Silica Dissolution in Southern Ocean Sediments, Quat Res, 37, 361–378, https://doi.org/10.1016/0033-5894(92)90073-R, 1992.

Rembauville, M., Manno, C., Tarling, G. A., Blain, S., and Salter, I.: Strong contribution of diatom resting spores to deep-sea carbon transfer in naturally iron-fertilized waters downstream of South Georgia, Deep Sea Res 1 Oceanogr Res Pap, 115, 22–35, https://doi.org/10.1016/j.dsr.2016.05.002, 2016.

Rigual-Hernández, A. S., Trull, T. W., Bray, S. G., Cortina, A., and Armand, L. K.: Latitudinal and temporal distributions of diatom populations in the pelagic waters of the Subantarctic and Polar Frontal zones of the Southern Ocean and their role in the biological pump, Biogeosciences, 12, 5309–5337, https://doi.org/10.5194/BG-12-5309-2015, 2015.

Robinson, R. S. and Sigman, D. M.: Nitrogen isotopic evidence for a poleward decrease in surface nitrate within the ice age Antarctic, Quat Sci Rev, 27, 1076–1090, https://doi.org/10.1016/j.quascirev.2008.02.005, 2008.

Robinson, R. S., Brunelle, B. G., and Sigman, D. M.: Revisiting nutrient utilization in the glacial Antarctic: Evidence from a new method for diatom-bound N isotopic analysis, Paleoceanography, 19, https://doi.org/10.1029/2003PA000996, 2004.

Robinson, R. S., Sigman, D. M., DiFiore, P. J., Rohde, M. M., Mashiotta, T. A., and Lea, D. W.: Diatom-bound 15N/14N: New support for enhanced nutrient consumption in the ice age subantarctic, Paleoceanography, 20, 1–14, https://doi.org/10.1029/2004PA001114, 2005.

Robinson, R. S., Jones, C. A., Kelly, R. P., Love, A., Closset, I., Rafter, P. A., and Brzezinski, M.: A Test of the Diatom-Bound Paleopr Tracing the Isotopic Composition of Nutrient-Nitrogen Into Southern Ocean Particles and Sediments, Global Biogeochem Cycles, 34, https://doi.org/10.1029/2019GB006508, 2020.

https://doi.org/10.5194/egusphere-2023-2564
Preprint. Discussion started: 16 November 2023
© Author(s) 2023. CC BY 4.0 License.

Rynearson, T. A., Richardson, K., Lampitt, R. S., Sieracki, M. E., Poulton, A. J., Lyngsgaard, M. M., and Perry, M. J.: Major contribution of diatom resting spores to vertical flux in the sub-polar North Atlantic, Deep Sea Research Part I: Oceanographic Research Papers, 82, 60–71, https://doi.org/10.1016/J.DSR.2013.07.013, 2013.

Sarmiento, J. L. and Toggweiler, J. R.: A new model for the role of the oceans in determining atmospheric pCO2, Nature, 308, 621–624, https://doi.org/10.1038/308621a0, 1984.

Scherer, R.: A new method for the determination of absolute abundance of diatoms and other silt-sized sedimentary particles, J Paleolimnol, 12, 171–179, 1994.

Schweitzer, P. N.: Monthly averaged polar sea-ice concentration, 1995.

Siegenthaler, U. and Wenk, T.: Rapid atmospheric CO2 variations and ocean circulation, Nature 1984 308:5960, 308, 624–626, https://doi.org/10.1038/308624a0, 1984.

Sigman, D. M. and Boyle, E. A.: Glacial/interglacial variations in atmospheric carbon dioxide, Nature 2000 407:6806, 407, 859–869, https://doi.org/10.1038/35038000, 2000.

Sigman, D. M., Altabet, M. A., Francois, R., McCorkle, D. C., and Gaillard, J. F.: The isotopic composition of diatom-bound nitrogen in Southern Ocean sediments, Paleoceanography, 14, 118–134, https://doi.org/10.1029/1998PA900018, 1999.

Sigman, D. M., Casciotti, K. L., Andreani, M., Barford, C., Galanter, M., and Böhlke, J. K.: A bacterial method for the nitrogen isotopic analysis of nitrate in seawater and freshwater, Anal Chem, 73, 4145–4153, https://doi.org/10.1021/AC010088E/ASSET/IMAGES/LARGE/AC010088EF00006.JPEG, 2001.

Sigman, D. M., Hain, M. P., and Haug, G. H.: The polar ocean and glacial cycles in atmospheric CO2 concentration, Nature 2010 466:7302, 466, 47–55, https://doi.org/10.1038/nature09149, 2010.

Smetacek, V., Klaas, C., Strass, V. H., Assmy, P., Montresor, M., Cisewski, B., Savoye, N., Webb, A., D'Ovidio, F., Arrieta, J. M., Bathmann, U., Bellerby, R., Berg, G. M., Croot, P., Gonzalez, S., Henjes, J., Herndl, G. J., Hoffmann, L. J., Leach, H., Losch, M., Mills, M. M., Neill, C., Peeken, I., Röttgers, R., Sachs, O., Sauter, E., Schmidt, M. M., Schwarz, J., Terbrüggen, A., and Wolf-Gladrow, D.: Deep carbon export from a Southern Ocean iron-fertilized diatom bloom, Nature 2012 487:7407, 487, 313–319, https://doi.org/10.1038/nature11229, 2012.

Strickland, J. and Parsons, T.: A practical handbook of seawater analysis, 2nd ed., Fisheries Research Board of Canada, Ottawa, Canada, 1972.

Studer, A. S., Ellis, K. K., Oleynik, S., Sigman, D. M., and Haug, G. H.: Size-specific opal-bound nitrogen isotope measurements in North Pacific sediments, Geochim Cosmochim Acta, 120, 179–194, https://doi.org/10.1016/j.gca.2013.06.041, 2013.

Studer, A. S., Sigman, D. M., Martínez-García, A., Benz, V., Winckler, G., Kuhn, G., Esper, O., Lamy, F., Jaccard, S. L., Wacker, L., Oleynik, S., Gersonde, R., and Haug, G. H.: Antarctic Zone nutrient conditions during the last two glacial cycles, Paleoceanography, 30, 845–862, https://doi.org/10.1002/2014PA002745, 2015.

Sumper, M. and Kröger, N.: Silica formation in diatoms: the function of long-chain polyamines and silaffins, J Mater Chem, 14, 2059–2065, https://doi.org/10.1039/B401028K, 2004.

https://doi.org/10.5194/egusphere-2023-2564
Preprint. Discussion started: 16 November 2023
© Author(s) 2023. CC BY 4.0 License.

Swann, G. E. A., Pike, J., Snelling, A. M., Leng, M. J., and Williams, M. C.: Seasonally resolved diatom δ18O records from the West Antarctic Peninsula over the last deglaciation, Earth Planet Sci Lett, 364, 12–23, https://doi.org/10.1016/J.EPSL.2012.12.016, 2013.

Taylor, F. and Sjunneskog, C.: Postglacial marine diatom record of the Palmer Deep, Antarctic Peninsula (ODP Leg 178, Site 1098) 2. Diatom assemblages, Paleoceanography, 17, PAL 2-1-PAL 2-12, https://doi.org/10.1029/2000PA000564, 2002.

Tesson, B., Lerch, S. J. L., and Hildebrand, M.: Characterization of a New Protein Family Associated With the Silica Deposition Vesicle Membrane Enables Genetic Manipulation of Diatom Silica, Scientific Reports 2017 7:1, 7, 1–13, https://doi.org/10.1038/s41598-017-13613-8, 2017.

Tréguer, P., Bowler, C., Moriceau, B., Dutkiewicz, S., Gehlen, M., Aumont, O., Bittner, L., Dugdale, R., Finkel, Z., Iudicone, D., Jahn, O., Guidi, L., Lasbleiz, M., Leblanc, K., Levy, M., and Pondaven, P.: Influence of diatom diversity on the ocean biological carbon pump, Nat Geosci, 11, 27–37, https://doi.org/10.1038/s41561-017-0028-x, 2018.

Wada, E. and Hattori, A.: Nitrogen isotope effects in the assimilation of inorganic nitrogenous compounds by marine diatoms, Geomicrobiol J, 1, 85–101, https://doi.org/10.1080/01490457809377725, 1978.

Zielinski, U. and Gersonde, R.: Diatom distribution in Southern Ocean surface sediments (Atlantic sector): Implications for paleoenvironmental reconstructions, Palaeogeogr Palaeoclimatol Palaeoecol, 129, 213–250, https://doi.org/10.1016/S0031-0182(96)00130-7, 1997.